Inorg. Chem. **2004**, *43*, 8626–8636

Tetra-2,3-pyrazinoporphyrazines with Externally Appended Pyridine Rings. 1. Tetrakis-2,3-[5,6-di(2-pyridyl)pyrazino]porphyrazine: A New Macrocycle with Remarkable Electron-Deficient Properties

Maria Pia Donzello,[†] Zhongping Ou,[‡] Fabrizio Monacelli,[†] Giampaolo Ricciardi,[§] Corrado Rizzoli,[||] Claudio Ercolani,*[,†] and Karl M. Kadish*[,‡]

Dipartimento di Chimica, Università degli Studi di Roma "La Sapienza", P.le A. Moro 5, I-00185 Roma, Italy, Department of Chemistry, University of Houston, Houston, Texas 77204-5003, Dipartimento di Chimica, Università della Basilicata, Via N. Sauro 85, I-85100, Potenza, Italy, and Dipartimento di Chimica Generale ed Inorganica, Università di Parma, Viale delle Scienze 1, I-43100 Parma, Italy

Received August 9, 2004

A new pyrazinoporphyrazine macrocycle carrying externally appended pyridine rings, tetrakis-2,3-[5,6-di(2-pyridyl)-pyrazino]porphyrazine (hydrated), $[Py_8TPyzPzH_2]\cdot 2H_2O$, was prepared in high yield by direct cyclotetramerization of the precursor, 2,3-dicyano-5,6-di(2-pyridyl)-1,4-pyrazine, $[(CN)_2Py_2Pyz]$, in the presence of 1,8-diazabicyclo-[5.4.0]undec-7-ene (DBU). The single-crystal X-ray structure of $[(CN)_2Py_2Pyz]$ shows a noncoplanar positioning of the pyrazine and pyridine rings in the two slightly different independent molecular units present in the crystal. UV–vis spectra of $[Py_8TPyzPzH_2]$ were measured in two nondonor solvents ($CHCl_3$, CH_2Cl_2), a slightly basic solvent (pyridine), and an acidic solvent (CH_3COOH). In all cases, the spectral changes are consistent with the occurrence of molecular aggregation and colloidal dispersions which break up with time to give clear solutions containing exclusively the monomeric form of the macrocycle, either neutral $[Py_8TPyzPzH_2]$ (in $CHCl_3$, CH_2Cl_2, and CH_3COOH) or dianionic $[Py_8TPyzPz]^{2-}$ (in pyridine). A spectrally monitored titration of $[Py_8TPyzPzH_2]$ in CH_2Cl_2 with TBA(OH) shows the loss of two protons from the macrocyclic core and quantitative conversion of $[Py_8TPyzPzH_2]$ to $[Py_8TPyzPz]^{2-}$. Cyclic voltammetry and thin-layer spectroelectrochemical measurements show that $[Py_8TPyzPzH_2]$ is present in CH_2Cl_2 while $[Py_8TPyzPz]^{2-}$ is present in pyridine, but both forms of the compound exhibit identical electrochemical behavior, consistent with a conversion of the dianion to the neutral porphyrazine in pyridine prior to electroreduction via four reversible one-electron transfer steps. No oxidations of the macrocycle are observed in either solvent containing 0.1 M tetrabuthylammonium perchlorate (TBAP). A comparison of the electrochemical behavior for $[Py_8TPyzPzH_2]$ with what is reported for related phthalocyanine and porphyrazine analogues highlights the remarkable electron-accepting properties of the presently investigated free-base macrocycle.

Introduction

The synthesis, characterization, and applications of tetrapyrrolic macrocycles such as porphyrins,[1] phthalocyanines,[2] and their aza-analogues are thoroughly studied areas of research. Porphyrazines (tetraazaporphyrins), which are derived from the tetraazaporphin skeleton and include phthalocyanines as the most widely investigated member of this family (see Scheme 1, I for the unmetalated species), have received comparatively less attention, although they are gaining progressively more interest.[3,4]

* To whom correspondence should be addressed. E-mail: claudio.ercolani@uniromal.it (C.E.); kkadish@uh.edu (K.M.K.).
[†] Università degli Studi di Roma "La Sapienza".
[‡] University of Houston.
[§] Università della Basilicata.
[||] Università di Parma.

(1) *The Porphyrin Handbook*; Kadish, K. M., Smith, K. M., Guilard, R., Eds.; Academic Press: New York, 2000; Vols. 1−10; 2003; Vols. 11−14.

(2) (a) *The Porphyrin Handbook*; Kadish, K. M., Smith, K. M., Guilard, R., Eds.; Academic Press: New York, 2003; Vols. 15−20. (b) *Phthalocyanines: Properties and Applications*; Leznoff, C. C., Lever, A. B. P., Eds.; VCH Publishers: New York, 1989−96; Vols. 1−4.

(3) Stuzhin, P. A.; Ercolani, C. *The Porphyrin Handbook*; Kadish, K. M., Smith, K. M., Guilard, R., Eds.; Academic Press: New York, 2003; Vol. 15, Chapter 101, pp 263−364.

10.1021/ic048909w CCC: $27.50
Published on Web 12/03/2004

Scheme 1. General Schematic Representation of Symmetrical Porphyrazine Macrocycles Carrying Annulated Rings[a]

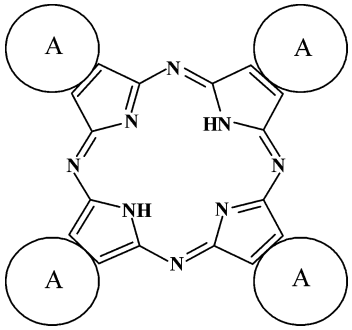

[a] I, Phthalocyanine, [PcH_2] (A = benzene); II, tetrakis(1,2,5-thiadiazolo)porphyrazine, [$TTDPzH_2$] (A = 1,2,5-thiadiazole); III, tetrakis(1,2,5-selenodiazolo)porphyrazine, [$TSeDPzH_2$] (A = 1,2,5-selenodiazole); IV, tetrakis(5,7-diphenyl-6*H*-1,4-diazepino)porphyrazine, [Ph_8DzPzH_2] (A = 5,7-diphenyl-6*H*-1,4-diazepine); V, tetrakis[5,6-di-(2-pyridyl)-pyrazino]porphyrazine, [$Py_8TPyzPzH_2$] (A = 5,6-di-(2-pyridyl)pyrazine).

As part of our studies on novel families of porphyrazines, we have reported molecular systems carrying peripherally annulated electron-deficient five-,[5,6] six-,[6a] and seven-membered[7] heterocycles. Tetrakis(1,2,5-thiadiazolo)- and tetrakis(1,2,5-selenodiazolo)porphyrazine (Scheme 1, II and III, respectively) and their metal derivatives[5,6] having N−S−N and N−Se−N triatomic fragments incorporated into the external five-membered heterocyclic rings resemble in many respects the phthalocyanine molecular framework (essentially square planar molecular geometry, same number of π-electrons, low solubility, high thermal stability, vaporizability). Recent X-ray work provides substantial additional information on the structural and electronic features of these symmetric porphyrazine macrocycles.[8] Moreover, the S- and Se-porphyrazines differ from the phthalocyanines in terms of (a) intramolecular π-electronic distribution due to the presence of the external electron-withdrawing thiadiazole or selenodiazole rings in place of the benzene rings, (b) chemical reactivity, as shown, for instance by the Se-porphyrazines in their reactions with H_2S,[6a] and (c) intermolecular contacts in the solid state, both for the crystalline[8] and the amorphous or quasiamorphous materials.[9] Furthermore, the formation of low symmetry macrocycles[10] has been reported for S- and Se-porphyrazines.

Also characterized is another class of porphyrazine macrocycles, tetrakis-2,3-(5,7-diphenyl-6*H*-1,4-diazepino)porphyrazine,[7] [Ph_8DzPzH_2] (Scheme 1, IV), and its metal complexes with nontransition and first-row transition metal ions, carrying peripherally annulated seven-membered diazepine rings. The structural features of these diazepinoporphyrazines are markedly different from those of the S- and Se-porphyrazines mentioned above, and from the phthalocyanines as well, for several reasons. First, they are far from being entirely planar, and hence, it was of interest to understand how the central essentially flat porphyrazine core and the peripheral nonplanar diazepine rings reciprocally interact, both structurally and electronically.[7b] In addition, the presence of the eight peripheral phenyl groups in the macrocycles leads to very specific physical properties, one of which is an increased solubility which may expand the spectrum of their possible practical applications.

In the present paper, we report the synthesis and characterization of a new member among the class of tetrakis-2,3-(pyrazino)porphyrazine and its peripherally substituted analogues.[3] The compound is tetrakis-2,3-[5,6-di(2-pyridyl)-pyrazino]porphyrazine, [$Py_8TPyzPzH_2$] (Scheme 1, V), which is obtained in a one-step autocyclotetramerization process from the precursor 2,3-dicyano-5,6-di(2-pyridyl)-1,4-pyrazine, [$(CN)_2Py_2Pyz$)], catalyzed by 1,8-diazabicyclo[5.4.0]-undec-7-ene (DBU).[11] The unmetalated "pyrazinoporphyrazine" macrocycle is normally obtained in the hydrated form, [$Py_8TPyzPzH_2$]·$2H_2O$. It exhibits adequate solubility in both polar and nonpolar solvents due to the presence of eight peripherally appended pyridine rings. As will be shown, the pyridine groups highly enhance the overall electron deficiency of the entire tetrapyrazinoporphyrazine macrocycle, which can also be seen as a promising material for the formation of aquo-soluble cationic porphyrazines, which are presently under detailed investigation. To our knowledge, there is to date only one class of similar cationic porphyrazines with externally appended pyridine rings reported in the literature.[12]

The following paper[13] expands upon the current work and describes the synthesis and characterization of a series of metal complexes of tetrakis-2,3-[5,6-di(2-piridyl)pyrazino]-porphyrazine, [$Py_8TPyzPzH_2$], having the general formula [$Py_8TPyzPzM$]·xH_2O ($M = Mg^{II}(H_2O)$, Mn^{II}, Co^{II}, Cu^{II}, Zn^{II}; $x = 3-8$) The Mg^{II} and Cu^{II} complexes of this macrocycle were only briefly reported[14] in an earlier paper from another laboratory and not characterized in detail.

Experimental Section

Solvents and reagents were used as purchased unless otherwise specified. Anhydrous tetrahydrofuran (THF) was prepared by

(4) Michel, S. L. J.; Hoffman, B. M.; Baum, S. M.; Barrett, A. G. M. *Progress in Inorganic Chemistry*; Karlin, K. D., Ed.; J. Wiley & Sons: New York, 2001; Vol. 50, pp 473−591.
(5) (a) Stuzhin, P. A.; Bauer, E. M.; Ercolani, C. *Inorg. Chem.* **1998**, *37*, 1533. (b) Bauer, E. M.; Cardarilli, D.; Ercolani, C.; Stuzhin, P. A.; Russo, U. *Inorg. Chem.* **1999**, *38*, 6114.
(6) (a) Bauer, E. M.; Ercolani, C.; Galli, P.; Popkova, I. A.; Stuzhin, P. A. *J. Porphyrins Phthalocyanines* **1999**, *3*, 371. (b) Angeloni, S.; Bauer, E. M.; Ercolani, C.; Popkova, I. A.; Stuzhin, P. A. *J. Porphyrins Phthalocyanines* **2001**, *5*, 881.
(7) (a) Donzello, M. P.; Ercolani, C.; Stuzhin, P. A.; Chiesi-Villa, A.; Rizzoli, C. *Eur. J. Inorg. Chem.* **1999**, 2075. (b) Donzello, M. P.; Dini, D.; D'Arcangelo, G.; Ercolani, C.; Zhan, R.; Ou, Z.; Stuzhin, P. A.; Kadish, K. M. *J. Am. Chem. Soc.* **2003**, *125*, 14190.
(8) (a) Fujimori, M.; Suzuki, Y.; Yoshikawa, H.; Awaga, K. *Angew. Chem., Int. Ed.* **2003**, *42*, 5863. (b) Suzuki, Y.; Fujimori, M.; Yoshikawa, H.; Awaga, K. *Chem. Eur. J.* **2004**, *10*, 5158.
(9) Caminiti, R.; Sadun, C.; Donzello, M. P.; Ercolani, C. Unpublished results.
(10) (a) Ercolani, C.; Kudrik, E. V.; Moraschi, S.; Popkova, I. A.; Stuzhin, P. A. First International Conference on Porphyrins and Phthalocyanines, Dijon, France, June 25−30, 2000, post 575. (b) Kudrik, E. V.; Bauer, E. M.; Ercolani, C.; Stuzhin, P. A.; Chiesi-Villa, A.; Rizzoli, C. *Mendeleev Commun.* **2001**, 45. (c) Donzello, M. P.; Ercolani, C.; Gaberkorn, A. A.; Kudrik, E. V.; Meneghetti, M.; Marcolongo, G.; Rizzoli, C.; Stuzhin, P. A. *Chem. Eur. J.* **2003**, *9*, 4009.
(11) Ohta, K.; Watanabe, T.; Fujimoto, T.; Yamamoto, I. *J. Chem. Soc., Chem. Commun.* **1989**, 1611.
(12) Anderson, M. E.; Barrett, A. G. M.; Hoffman, B. M. *Inorg. Chem.* **1999**, *38*, 6143.
(13) Part 2: Donzello, M. P.; Ou, Z.; Dini, D.; Meneghetti, M.; Ercolani, C.; Kadish, K. M. *Inorg. Chem.* **2004**, *43*, 8637−8648.
(14) Mørkved, E. H.; Ossleten, H.; Kjøsen, H.; Bjørlo, O. *J. Prakt. Chem.* **2000**, *342*, 83.

refluxing it over potassium and then distilling it before use. Pyridine was dried by reflux over CaO. Dimethyl sulfoxide (DMSO) was freshly distilled over CaH_2. Diaminomaleonitrile and 2,2′-pyridil were purchased from Aldrich and used without further purification. Tetrabuthylammonium hydroxide (TBA(OH)) was purchased from Aldrich and used as received.

2,3-Dicyano-5,6-di-(2-pyridyl)-1,4-pyrazine, [$(CN)_2Py_2Pyz$)]. The synthesis of [$(CN)_2Py_2Pyz$], reported elsewhere,[14] was carried out in this work in a different manner and is as follows: 2,2′-pyridil (6.67 g, 31.4 mmol) and diaminomaleonitrile (3.84 g, 35.5 mmol) were added to THF (100 mL) in a 250 mL flask, and the mixture was kept refluxing for 2 h in an inert atmosphere. After cooling and addition of Na_2SO_4 followed by filtration, the brown solution which separated was brought to dryness by using a rotary evaporator. The solid residue obtained was washed repeatedly with hot water and brought to constant weight under vacuum (10^{-2} mmHg). Crystallization from hot toluene and hexane gave the desired species as a white material (mp 174 °C; 5.33 g, yield 60%). Calcd for $C_{16}H_8N_6$: C, 67.61; H, 2.81; N, 29.57. Found: C, 67.79; H, 2.75; N, 29.43%. Crystallization from CH_3OH led to single crystals suitable for X-ray work (see below). IR (cm^{-1}): 1588 vs, 1571 s, 1522 s, 1472 s, 1438 s, 1396 sh, 1385 vvs, 1298 w, 1283 m, 1274 w, 1234 m, 1225 sh, 1200 s, 1159 sh, 1153 m, 1130 s, 1096 vs, 1048 m, 995 vvs, 975 w, 960 w, 951 w, 903 sh, 895 m, 824 m, 793 vvs, 787 sh, 756 sh, 741 vvs, 711 w, 701 m, 694 w, 676 m, 624 vs, 607 m, 574 vvs, 533 vs, 499 w, 446 s, 404 s. ^1H NMR ($CDCl_3$, 293 K): δ/ppm = 8.22 (d, J = 3.68 Hz, 2 H; α,α' in Figure 4A), 7.95 (d, J = 7.93 Hz, 2 H; δ,δ'), 7.81 (dd, J = 7.70, 7.81 Hz, 2H; γ,γ'), 7.27 (dd, J = 4.41, 6.16 Hz, 2H; β,β').

Tetrakis-2,3-[5,6-di-(2-pyridyl)-pyrazino]porphyrazine, [$Py_8TPyzPzH_2$]·$2H_2O$. The pyrazinoporphyrazine macrocycle was directly obtained by autocyclotetramerization of the precursor [$(CN)_2Py_2Pyz$] as follows: a thick test tube containing [$(CN)_2Py_2Pyz$] (3.04 g, 10.8 mmol) was heated in an oil bath at a temperature of 180 °C. A few drops of DBU were added as catalyst,[11] and the mixture was manually stirred until it was almost completely solidified. After cooling, the solid material was finely ground and purified by Soxhlet extraction with CH_3OH (10−15 h) and then with acetone (10 h) to remove the unreacted monomer and other contaminants. The dark green residual powder was brought to constant weight under vacuum (10^{-2} mmHg) (2.03 g, yield 66%). TGA shows an overall weight loss of 3.33% (calcd for two molecules of water: 3.07%). Calcd for [$Py_8TPyzPzH_2$]·$2H_2O$, $C_{64}H_{38}N_{24}O_2$: C, 65.41; H, 3.26; N, 28.60. Found: C, 65.84; H, 3.08; N, 28.34%. MS (FAB), m/z (%): 1138 (100) [$Py_8TPyzPzH_2$−H]$^+$ (see Figure S3). IR (cm^{-1}): 3293 w, 3055 w, 3003 vw, 1741 w, 1694 vw, 1630 w, 1586 s, 1568 m, 1542 m, 1502 m, 1471 s, 1432 m, 1382 w, 1361 vs, 1322 w, 1292 vw, 1278 w, 1236 vs, 1229 vs, 1174 w, 1145 vs, 1106 s, 1094 s, 1066 m, 1044 m, 1015 s, 994 vs, 951 vs, 892 w, 830 m, 793 s, 763 vs, 746 vs, 719 vw, 705 vvs, 699 vvs, 650 vs, 629 m, 607 w, 598 m, 554 m, 531 vw, 504 vw, 492 sh, 460 vw, 437 m, 404 m (Figure S4). ^1H NMR ($CDCl_3$, 293 K): δ/ppm = 8.71 (d, J = 7.87 Hz, 8H; δ,δ' in Figure 4B), 8.38 (d, J = 5.04 Hz, 8H; α,α'), 8.03 (dd, J = 6.13, 7.87 Hz, 8H; γ,γ'), 7.33 (dd, J = 6.13, 6.50 Hz, 8H; β,β'), −0.68 (broad s, 2H (HN)).

Thermogravimetric analysis on different samples of the macrocycle shows that the amount of clathrated water is sometimes higher than for the formulation given above and is often indicative of the presence of up to three water molecules. Complete elimination of water was accomplished by heating the solid under vacuum (10^{-2} mmHg) at 100 °C for 1 h. Calcd for [$Py_8TPyzPzH_2$], $C_{64}H_{34}N_{24}$: C, 67.48; H, 3.01; N, 29.50. Found: C, 67.00; H, 3.01; N, 29.05%.

Further purification of the hydrated macrocycle [$Py_8TPyzPzH_2$]·$2H_2O$, obtained as described above, was required in order to obtain a clean UV−vis spectrum. Impure samples showed the presence of an absorption at ca. 300 nm due to small amounts of the precursor and/or other contaminants present. When this was the case, the macrocycle was then suspended in CH_2Cl_2 which dissolved the contaminant material (together with some amount of the macrocycle). The undissolved material was then separated by centrifugation and brought to constant weight under vacuum. Room temperature magnetic susceptibility measurements indicate [$Py_8TPyzPzH_2$]·$2H_2O$ to be diamagnetic, as expected. The magnetic molar susceptibility measured directly on the macrocycle gave the value $\chi_M = -629 \times 10^{-6}$ cgsu, in good agreement with the value calculated by using the Pascal's constants (-607×10^{-6} cgsu) and that obtained by taking four times the value measured directly on a highly purified sample of the precursor, [$(CN)_2Py_2Pyz$] (-155×10^{-6} cgsu).

X-ray Crystallography of the Precursor [$(CN)_2Py_2Pyz$]. Crystal data and details associated with structure refinement are given in the Supporting Information. Relevant conformation parameters are quoted in Table S6. Data were collected on an Enraf-Nonius CAD4 diffractometer using graphite-monochromatized Cu Kα radiation at 298 K. Solution and refinement were carried out using the programs SIR97[15] and SHELX93.[16]

Electrochemical and Spectroelectrochemical Measurements. Cyclic voltammetry (CV) measurements were performed at 298 K on an EG&G model 173 potentiostat coupled with an EG&E model 175 universal programmer in CH_2Cl_2 (Fluka) or pyridine (Aldrich, anhydrous, 99.8%) containing 0.1 M tetrabutylammonium perchlorate (TBAP) as supporting electrolyte. High purity N_2 from Trigas was used to deoxygenate the solution before each electrochemical experiment. TBAP was purchased from Sigma Chemical or Fluka Chemika Co., recrystallized from ethyl alcohol and dried under vacuum at 40 °C for at least one week prior to use. A three electrode system was used and consisted of a glassy carbon working electrode, a platinum wire counter electrode, and a saturated calomel reference electrode (SCE). The reference electrode was separated from the bulk of the solution by a fritted-glass bridge filled with the solvent/supporting electrolyte mixture. Thin-layer spectroelectrochemistry measurements were carried out with an optically transparent platinum thin-layer working electrode using a Hewlett-Packard model 8453 diode array spectrophotometer coupled with an EG&G model 173 universal programmer. These measurements were carried out in solutions containing 0.2 M TBAP as supporting electrolyte. EPR spectra, taken in association with electrochemical measurements, were obtained with an IBM model ESP 300 apparatus.

Other Physical Measurements. IR spectra were taken with a Perkin-Elmer 1760 X spectrophotometer in the range 4000−400 cm^{-1} by using KBr pellets. Except for the case of spectroelectrochemistry (see above), all UV−vis solution spectra were recorded with a Varian Cary 5E spectrometer. Thermogravimetric analyses (TGA) were performed on a Stanton Redcroft model STA-781 analyzer under an N_2 atmosphere (0.5 L/min). FAB experiments were carried out on a multiple quadrupole instrument (VG quattro). Elemental analyses for C, H, and N were provided by the "Servizio di Microanalisi" at the Dipartimento di Chimica, Università "La Sapienza" (Rome), on an EA 1110 CHNS-O instrument. X-ray powder diffraction patterns were obtained on a Philips PW 1710 diffractometer by using Cu Kα (Ni-filtered) radiation. Room

(15) Altomare, A.; Burla, M. C.; Camalli, M.; Cascarano, G.; Giacovazzo, C.; Guagliardi, A.; Moliterni, A. G. G.; Polidori, G.; Spagna, R. *J. Appl. Crystallogr.* **1999**, *32*, 115.
(16) Sheldrick, G. M. *SHELXL93*: *Program for crystal structure refinement*; University of Göttingen: Göttingen, Germany, 1993.

Table 1. Experimental Data for the X-ray Diffraction Study on Crystalline $[(CN)_2Py_2Pyz]$

compd	$[(CN)_2Py_2Pyz]$
formula	$C_{16}H_8N_6$
a, Å	16.977(3)
b, Å	8.126(2)
c, Å	20.628(5)
V, Å^3	2845.7(11)
Z	8
fw	284.3
space group	*Pna*2$_1$ (No. 33)
T, °C	25
λ, Å	1.54178
ρ_{calc}, g cm^{-3}	1.327
μ, cm^{-1}	6.98
transm coeff	0.954−1.000
R^a	0.035
wR_2	0.096
GOF	0.909
N-observed[b]	2299
N-independent[c]	2774
N-refinement[d]	2774
variables	398

[a] Calculated on the observed reflections having $I > 2\sigma(I)$. [b] No. obsd is the number of the independent reflections having $I > 2\sigma(I)$. [c] *N*-independent is the number of independent reflections. [d] *N*-refinement is the number of reflection used in the refinement having $I > 0$.

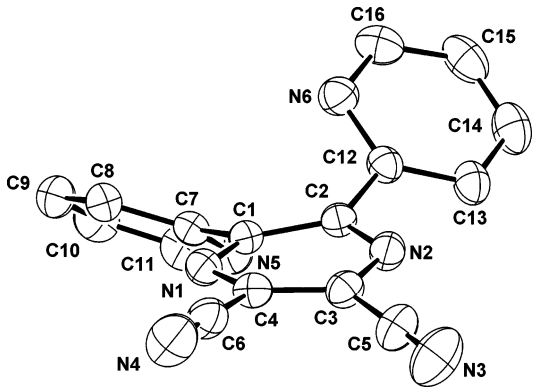

Figure 1. ORTEP front-view (30% probability ellipsoids) of molecule A in $[(CN)_2Py_2Pyz]$.

temperature magnetic susceptibility measurements were carried out by the Gouy method using a $NiCl_2$ solution as calibrant. ^{1}H NMR spectra were recorded on a 200 MHz Bruker spectrophotometer at the Dipartimento di Chimica, Università "La Sapienza" (Rome).

Results and Discussion

(A) $[(CN)_2Py_2Pyz]$. X-ray Data. Crystal data on 2,3-dicyano-5,6-di(2-pyridyl)-1,4-pyrazine are listed in Table 1. The structure consists of two crystallographically independent molecules (labeled A and B) showing a very similar geometry. Figure 1 shows the ORTEP front-view of molecule A. In this molecule, and in B as well, the pyrazine rings are slightly distorted, assuming a twist-boat conformation as indicated by the parameters given in Table S6 (Supporting Information). Selected bond distances and angles, given in Table 2, are as expected. The planes of the two pyridine rings are rotated with respect to the mean plane of the pyrazine ring by 38.3(1)° and 36.6(1)° in molecule A and by 37.0(1)° and 43.0(1)° in molecule B. One pyridine ring is rotated with respect to the other one by 56.3(1)° and 58.4(1)° in molecules A and B, respectively.

Table 2. Selected Bond Distances (Å) and Angles (deg) for $[(CN)_2Py_2Pyz]$

	molecule A	molecule B
N(1)−C(1)	1.333(3)	1.340(3)
N(1)−C(4)	1.336(3)	1.344(4)
N(2)−C(2)	1.324(3)	1.330(3)
N(2)−C(3)	1.337(4)	1.333(3)
N(3)−C(5)	1.133(6)	1.141(5)
N(4)−C(6)	1.137(5)	1.140(6)
C(1)−C(2)	1.426(3)	1.421(4)
C(1)−C(7)	1.482(3)	1.476(4)
C(2)−C(12)	1.486(3)	1.484(3)
C(3)−C(4)	1.387(4)	1.379(5)
C(3)−C(5)	1.445(5)	1.439(5)
C(4)−C(6)	1.443(5)	1.443(5)
C(1)−N(1)−C(4)	118.1(2)	117.7(2)
C(2)−N(2)−C(3)	117.9(2)	118.3(2)
N(1)−C(1)−C(2)	119.8(2)	119.8(2)
N(1)−C(1)−C(7)	116.3(2)	117.0(2)
C(2)−C(1)−C(7)	123.8(2)	123.1(3)
N(2)−C(2)−C(1)	120.3(2)	120.4(2)
N(2)−C(2)−C(12)	117.3(2)	115.2(2)
C(1)−C(2)−C(12)	122.4(2)	124.3(2)
N(2)−C(3)−C(4)	121.2(3)	121.0(2)
N(2)−C(3)−C(5)	118.5(2)	117.0(2)
C(4)−C(3)−C(5)	120.3(2)	121.9(3)
N(1)−C(4)−C(3)	120.7(2)	121.3(3)
N(1)−C(4)−C(6)	118.1(2)	118.3(2)
C(3)−C(4)−C(6)	121.2(3)	120.4(2)
N(3)−C(5)−C(3)	178.2(4)	178.5(4)
N(4)−C(6)−C(4)	179.4(4)	176.9(4)

Despite the lack of coplanarity, some limited form of π-conjugation occurs between the pyrazine and pyridine rings as indicated (Table 2) by the C(1)−C(7) bond distances (1.482(3) Å in A, 1.476(4) Å in B) and the C(2)−C(12) bond distances (1.486(3) Å in A and 1.484(3) Å in B) which are a little shorter than those of typical C−C σ bonds (1.53 Å).[17] In the crystal packing of $[(CN)_2Py_2Pyz]$, intermolecular contacts can be interpreted in terms of weak hydrogen bond interactions mainly involving the nitrogen atoms of the cyano groups and CH groups from adjacent pyridine rings: N(3)A···H(16)A′, 2.90 Å; N(3)A···C(16)A′, 3.731(6) Å; N(3)A···H(16)A′−C(16)A′, 150°; N(3)A···H(16)B″, 2.87 Å; N(3)A···C(16)B″, 3.534(5) Å; N(3)A···H(16)B″−C(16)B″, 129°; N(4)B···H(14)B*, 2.84 Å; N(4)B···C(14)B*, 3.767(6) Å; N(4)B···H(14)B*−C(14)B*, 178° (prime, double prime, and asterisk refer to transformations of $1 - x$, $-y$, $0.5 + z$; x, $1 + y$, z; $1 - x$, $1 - y$, $0.5 + z$, respectively).

(B) $[Py_8TPyzPzH_2]$. Synthetic Aspects. The hydrated macrocycle $[Py_8TPyzPzH_2]\cdot 2H_2O$ is obtained as a substantially amorphous solid material (see its X-ray powder pattern in Figure S5). The water molecules can be eliminated by mild heating ($T < 100$ °C) under vacuum. After the loss of water, thermogravimetric analysis shows that the macrocycle is stable in an inert atmosphere at temperatures up to ca. 300 °C. Exposure of the heated sample to air leads to a rehydration of the material. Figure 2 shows a schematic perspective view of $[Py_8TPyzPzH_2]$ (hereafter water molecules will be neglected in the compound structure, unless strictly required). In depicting the orientation of the molecule $[Py_8TPyzPzH_2]$, structural information on the precursor has been considered for each dipyridinopyrazine fragment,

(17) Allen, F. H.; Kennard, O.; Watson, D. G.; Brammer, L.; Orpen, A. G.; Taylor, R. *J. Chem. Soc., Perkin Trans* **1987**, *2*, S1.

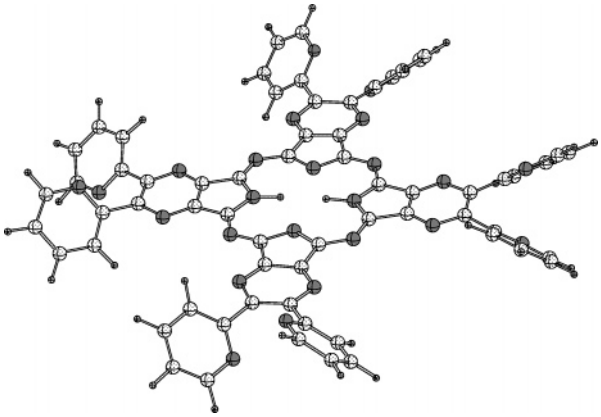

Figure 2. Schematic arbitrary representation of the macrocycle [$Py_8TPyzPzH_2$].

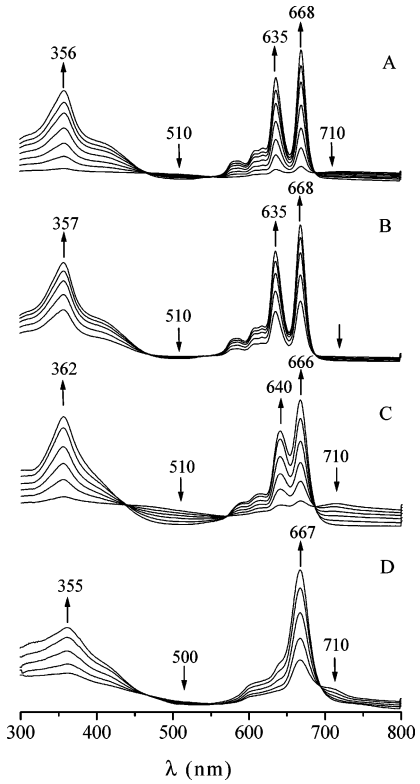

Figure 3. UV−vis spectra as a function of time for [$Py_8TPyzPzH_2$] in (A) $CHCl_3$, (B) CH_2Cl_2, (C) CH_3COOH, (D) pyridine.

assuming as practically unchanged the reciprocal orientation of the pyridine molecules relative to the plane of the respective pyrazine rings (see Figure 1).

UV−Vis Spectra. [$Py_8TPyzPzH_2$] is not easily dissolved in nondonor solvents ($CHCl_3$, CH_2Cl_2), slightly basic solvents (pyridine), or acidic solvents (CH_3COOH) but rather leads to the formation of turbid solutions due to aggregation by the macrocycle. In $CHCl_3$, the "colloidal" solution takes ca. 20 h before it becomes completely clear.

Figure 3A shows the UV−vis spectral behavior observed immediately after preparation of the solution. The initial spectrum is quite featureless over the region 300−800 nm, showing only a broad low intensity absorption centered at ca. 710 nm. However, the turbidity vanishes, and changes in the UV−vis spectrum are observed as a function of time; these consist of the appearance of two sharp intense peaks in the Q-band region at 635 and 668 nm, low-intensity peaks at ca. 580 (broad) and 609 and 618 nm and a peak in the Soret region at 356 nm (shoulder at ca. 400 nm). Concomitantly, the absorption at ca. 710 nm progressively decreases in intensity and finally disappears. Isosbestic points are clearly evidenced at ca. 450, 550, and 680 nm. The narrow intense Q-band peaks in the final spectrum indicate formation of a monomeric macrocycle in solution. A similar trend of spectral changes is also observed in CH_2Cl_2 (Figure 3B), where complete dissolution of the colloid is faster, generally occurring in ca. 1−2 h. The final spectrum closely resembles what is observed in $CHCl_3$ with the two Q-band peaks identically positioned (635 and 668 nm). This final spectrum is of the type normally observed for porphyrazines and phthalocyanines, showing Q (600−700 nm) and B bands (300−450 nm) due to the HOMO−LUMO $\pi-\pi^*$ transitions.[18,19] Moreover, due to the presence of the two central N−H groups, the symmetry of the central tetrapyrazinoporphyrazine core of [$Py_8TPyzPzH_2$] is D_{2h} (assuming as negligible the effect on the symmetry of the peripheral pyridine rings), and a split Q absorption is expected, in keeping with the findings. The peaks at 668 and 635 nm are assigned, respectively, as $a_u \rightarrow b_{2g}$ (Q_x) and $a_u \rightarrow b_{3g}$ (Q_y). The peak at 357 nm can be assigned as the B-band (unsplit, as is commonly observed), and the shoulder at ca. 400 nm is tentatively assigned to the $n \rightarrow \pi^*$ transition.[18,19]

Figure 3C illustrates the spectral changes which occur as a function of time in CH_3COOH. The spectral changes resemble closely what is observed in $CHCl_3$ and CH_2Cl_2 in that a splitting of the Q band for the monomer is maintained, indicative of D_{2h} symmetry. The final spectrum is therefore assigned to neutral [$Py_8TPyzPzH_2$] as expected due to the nature of the solvent. Obviously, some form of interaction between CH_3COOH with the eight pyridine rings and, to a minor extent, with the pyrazine parts of the macrocycle, as well as with the meso N atoms of the compound, is expected to occur, but this apparently has little effect on the UV−vis spectrum.

A colloidal solution is also formed in pyridine. The observed spectral variations as a function of time (ca. 20 h) are shown in Figure 3D. Unlike what is seen in the other solvents, the spectral changes in the Q-band region show the appearance of a single symmetrical narrow intense peak at 667 nm. This implies D_{4h} symmetry for the macrocycle and clearly suggests formation of the dianion $[Py_8TPyzPz]^{2-}$ consequent to deprotonation of the central NH groups. This deprotonation is further confirmed by titration experiments with TBA(OH) as described in later sections of this paper.

Qualitative and quantitative data are summarized in Table 3. The presence of clearly observed isosbestic points in Figure 3A−D might be taken as indicating a conversion of

(18) (a) Stillman, M. J. In *Phthalocyanines: Properties and Applications*; Leznoff, C. C., Lever, A. B. P., Eds.; VCH Publishers: New York, 1989; Vol. 1, pp 133−289. (b) Mack, J.; Stillman, M. J. In *The Porphyrin Handbook*; Kadish, K. M., Smith, K. M., Guilard, R., Eds.; Academic Press: New York, 2003; Vol. 16, pp 43−116.

(19) Gouterman, M. In *The Porphyrins*, Dolphin, D., Ed.; Academic Press: New York, 1978; Vol. III and references therein.

Table 3. UV−Vis Spectral Data (λ [nm] (log ϵ^a)) for [$Py_8TPyzPzH_2$] in Different Solvents

absorbing species	solvent	Soret region			Q-band region			
[$Py_8TPyzPzH_2$]	$CHCl_3$	356 (5.05)	400 (sh)	582 (4.40)	609 (4.57)	618 (4.61)	635 (5.10)	668 (5.21)
	CH_2Cl_2	357 (5.16)	400 (sh)	583 (4.54)	609 (4.69)	618 (4.72)	635 (5.21)	668 (5.30)
	CH_3COOH	355 (5.27)	386 (sh)	589 (4.60)		613 (4.74)	640 (5.21)	666 (5.31)
	C_6H_5CN[b]					623 (sh)	643	670
[$Py_8TPyzPz]^{2-}$	py	362 (4.83)	402 (sh)		605 (4.39)		643 (sh)	667 (5.06)
	DMSO[b]	362	402 (sh)		607		635 (sh)	664
	DMF[b]	360	402 (sh)		606		632 (sh)	662
	CH_3CN[b]					614 (sh)	627 (sh)	661

[a] ϵ values measured for the final monomeric form. [b] Qualitative spectra.

a precise aggregated species, supposedly a dimer into the monomer either neutral or anionic. The formation of dimers is a well-known phenomenon and is quite often observed for porphyrins,[20] phthalocyanines,[21,22] and porphyrazines,[3,8] occurring both in the solid state and in solution. Dimerization, which implies most usually a face-to-face molecular association involving $\pi-\pi$ interaction, may concern positively charged molecular units,[21] neutral species,[3,8,21] or anionic macrocyclic fragments.[21c,d] Unfortunately, the initial UV−vis spectra of [$Py_8TPyzPzH_2$] are very poorly defined, and it cannot be ruled out on the basis of these data alone that the ultimately formed monomeric species might originate from some combination of oligomeric forms, dimers included, which are responsible for the initial featureless spectra. However, additional information on this point is given by the ^{1}H NMR, cyclic voltammetric, and spectroelectrochemical data which provide a more detailed depiction of the solution behavior for the free-base macrocycle. This is described below.

^{1}H NMR Spectra. The room temperature ^{1}H NMR spectrum of a clear solution of [$Py_8TPyzPzH_2$] was obtained in $CDCl_3$ preliminarily passed through a column of neutral alumina (the final UV−vis spectrum was as expected for the monomeric form, $c \cong 10^{-4}$ M). Figure 4 shows the ^{1}H NMR spectrum of [$Py_8TPyzPzH_2$] in $CDCl_3$ and also includes that of the precursor [$(CN)_2Py_2Pyz$] for comparison. A resonance peak of [$Py_8TPyzPzH_2$] (Figure 4B, inset) is located at −0.68 ppm and is assigned to the two protons of the central NH groups. In comparing parts A and B of Figure 4, it is interesting to observe that, consequent to the formation of the macrocycle, the π-ring current induces a low field shift of all resonance peaks of the pyridine rings, the magnitude of this shift depending upon the distance of the protons from the central macrocycle. The β,β' protons, which are located further away, experience a shift of only 0.06 ppm. The α,α' and γ,γ' protons, which are more closely located, are shifted by 0.16 and 0.22 ppm, respectively. The δ,δ' protons, being in the closest position to the central π-conjugated system, are shifted by 0.76 ppm. This clearly indicates that the deshielding effect of the macrocycle on the δ,δ' protons overcomes the influence of the pyridine N-atom on the α,α' protons. As a consequence, an inversion of the position of the α,α' and δ,δ' proton resonances is observed (see arrows in Figure 4).

Electrochemical Measurements. Figure 5 shows cyclic voltammograms of [$Py_8TPyzPzH_2$] in CH_2Cl_2 and pyridine containing 0.1 M TBAP. A suspended excess of the com-

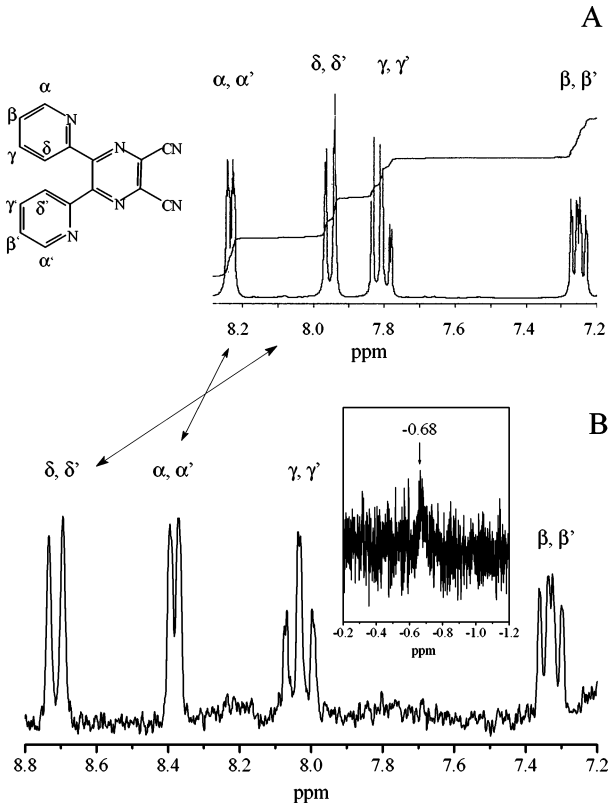

Figure 4. ^{1}H NMR spectra in $CDCl_3$ at 298 K of (A) [$(CN)_2Py_2Pyz$] (the spectrum shows two doublets at $\delta = 8.22$ and 7.95 ppm and two double doublets centered at $\delta = 7.81$ and 7.27 ppm), and (B) [$Py_8TPyzPzH_2$] (two doublets at $\delta = 8.71$ and 8.38 ppm and two double doublets centered at $\delta = 8.03$ and 7.33 ppm are observed). The inset shows the resonance of the protons of the central NH groups located at −0.68 ppm.

(20) Harvey, P. D. *The Porphyrin Handbook*; Kadish, K. M., Smith, K. M., Guilard, R., Eds.; Academic Press: New York, 2003; Vol. 18, Chapter 113, pp 63−243.
(21) (a) Lever, A. B. P.; Milaeva, E. R.; Speier, G. *Phthalocyanines Properties and Applications*; Leznoff, C. C., Lever, A. B. P., Eds.; VCH Publishers: New York, 1993; Vol. 3, pp 1−69. (b) L'Her, M.; Pondaven, A. *The Porphyrin Handbook*; Kadish, K. M., Smith, K. M., Guilard, R., Eds.; Academic Press: New York, 2003; Vol. 16, Chapter 104, pp 117−169. (c) Stillman, M. J. *Phthalocyanines Properties and Applications*; Leznoff, C. C., Lever, A. B. P., Eds.; VCH Publishers: New York, 1993; Vol. 3, pp 227−296. (d) Mack, J.; Stillman, M. J. In *The Porphyrin Handbook*; Kadish, K. M., Smith, K. M., Guilard, R., Eds.; Academic Press: New York, 2003; Vol. 16, Chapter 103, pp 43−116.
(22) For a general approach to phthalocyanine aggregation, also referred to the dimer formation, see: Snow, A. W. *The Porphyrin Handbook*; Kadish, K. M., Smith, K. M., Guilard, R., Eds.; Academic Press: New York, 2003; Vol. 17, Chapter 109, pp 129−173.
(23) Clack, D. W.; Hush, N. S.; Woolsey, I. S. *Inorg. Chim. Acta* **1976**, *19*, 129.

pound was required to obtain a sufficient concentration for the electrochemical measurements, but the presence of the colloid and excess undissolved bulk solid did not affect the voltammetric response, as indicated by the fact that five well-defined redox processes are observed in each solvent. No oxidations were observed up to a positive potential of 1.1 V versus SCE in pyridine or 1.8 V versus SCE in CH_2Cl_2. This is also the case for diazepinoporphyrazine as recently reported[7b] and was expected for $[Py_8TPyzPzH_2]$ due to the high acidity of the macrocycle (see below) which is easily reduced and hence difficult to oxidize.

Free-base phthalocyanine and its substituted derivatives are known to undergo up to four ring-centered reductions.[21a,23] A minimum of four ring-centered reductions are also observed for $[Ph_8DzPzH_2]$,[7b] and the same number of processes are therefore expected in the case of $[Py_8TPyzPzH_2]$. As seen in Figure 5, five reductions are obtained for $[Py_8TPyzPzH_2]$ in CH_2Cl_2 or pyridine by "regular" cyclic voltammetry at a scan rate of 100 mV/s. However, the third process (at -0.93 to -1.0 V vs SCE) is actually due to the reduction of dianionic $[Py_8TPyzPz]^{2-}$ which is in equilibrium with the neutral form of the porphyrazine as shown in eq 1.

$$[Py_8TPyzPzH_2] \rightleftarrows [Py_8TPyzPz]^{2-} + 2H^+ \qquad (1)$$

The UV−vis spectroscopic data in Figure 3 show clearly that $[Py_8TPyzPzH_2]$ is actually present in pyridine as $[Py_8TPyzPz]^{2-}$, and thus, the electrochemical data in both pyridine and CH_2Cl_2 are consistent with a reassociation of the two central protons to give $[Py_8TPyzPzH_2]$ prior to electron transfer via eqs 2−5.

$$[Py_8TPyzPzH_2] + e^- \rightleftarrows [Py_8TPyzPzH_2]^- \qquad (2)$$

$$[Py_8TPyzPzH_2]^- + e^- \rightleftarrows [Py_8TPyzPzH_2]^{2-} \qquad (3)$$

$$[Py_8TPyzPzH_2]^{2-} + e^- \rightleftarrows [Py_8TPyzPzH_2]^{3-} \qquad (4)$$

$$[Py_8TPyzPzH_2]^{3-} + e^- \rightleftarrows [Py_8TPyzPzH_2]^{4-} \qquad (5)$$

In parallel with these reactions, a reduction of the dianionic porphyrazine generated via the equilibrium in eq 1 is also observed, and this electrode reaction is given by eq 6.

$$[Py_8TPyzPz]^{2-} + e^- \rightleftarrows [Py_8TPyzPz]^{3-} \qquad (6)$$

It is important to point out that the $E_{1/2}$ values for the first and second reductions of $[Py_8TPyzPzH_2]$ differ by only 20 mV between CH_2Cl_2 and pyridine (see Figure 5), thus indicating that the same electroactive species, $[Py_8TPyzPzH_2]$ and $[Py_8TPyzPzH_2]^-$, must be stepwise reduced at the electrode in each solvent.

The equilibrium given by eq 1 can be documented by a variety of experiments, one of which is thin-layer cyclic voltammetry where the third reduction disappears upon going from a scan rate of 50 mV/s to a slower scan rate of 10 mV/s. This is shown in Figure 6, which displays five reductions at the higher scan rate and only four at the lower one where $[Py_8TPyzPz]^{2-}$ ($E_{1/2} = -0.93$ V) is converted to the more easily reduced $[Py_8TPyzPzH_2]$ ($E_{1/2} = -0.17$ V) at the lower scan rates. The first and last reductions show decreased currents at the lower scan rates, suggesting the presence of other equilibria under the application of an applied potential, but these were not investigated in further detail.

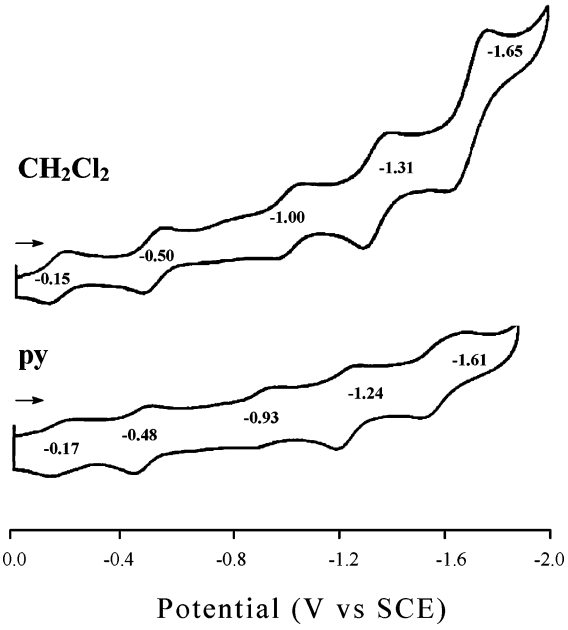

Figure 5. Cyclic voltammograms, with added $E_{1/2}$ values, of $[Py_8TPyzPzH_2]$ in CH_2Cl_2 ($[Py_8TPyzPzH_2]$ largely prevalent) and in pyridine ($[Py_8TPyzPz]^{2-}$ species mostly present), 0.1 M TBAP, scan rate = 100 mV/s.

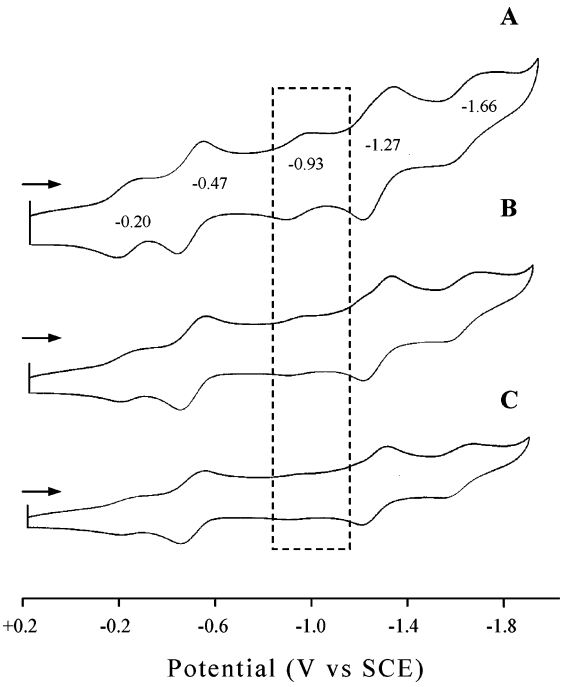

Figure 6. Thin-layer cyclic voltammograms (TLCVs) of $[Py_8TPyzPzH_2]$ in py, 0.2 M TBAP, at a scan rate of (A) 50 mV/s, (B) 20 mV/s, and (C) 10 mV/s.

The potential for reduction of $[Py_8TPyzPz]^{2-}$ (eq 6) occurs at -1.00 V in CH_2Cl_2 and -0.93 V in pyridine (Figure 5), and these values may be compared with an $E_{1/2} = -0.98$ V for the first reduction of the same compound in CH_2Cl_2 containing 0.135 M TBA(OH) (Figure 7).

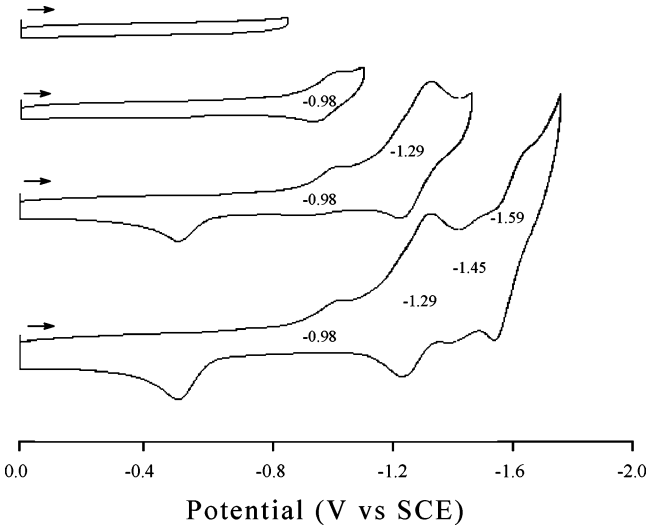

Figure 7. Cyclic voltammograms of $[Py_8TPyzPz]^{2-}$ in CH_2Cl_2, 0.1 M TBAP and 0.135 M TBA(OH).

In order to further investigate the equilibrium shown in eq 1, cyclic voltammograms were taken of $[Py_8TPyzPzH_2]$ in CH_2Cl_2 containing TBAP and added OH^- in the form of TBA(OH). Under these experimental conditions, the equilibrium in eq 1 is completely shifted to the right. Only the dianion $[Py_8TPyzPz]^{2-}$ is present in solutions of TBA(OH), and its reduction occurs as shown by eq 6. This is illustrated in Figure 7 where the dianion undergoes the first reduction at $E_{1/2} = -0.98$ V, a value coincident with the $E_{1/2}$ value observed in pure CH_2Cl_2 or pyridine (Figure 5).

Three further reductions of $[Py_8TPyzPz]^{2-}$ are observed in Figure 7 at more negative potentials, i.e., at -1.29, -1.45, and -1.59 V. The complete absence of the two reductions at positive potentials in the presence of TBA(OH), i.e., at ca. -0.15 and ca. -0.48 V, strengthens the conclusion that these processes are assigned as the first and second reductions of the free-base neutral macrocycle, $[Py_8TPyzPzH_2]$. Still referring to Figure 5, it must be considered that the two reductions occurring in CH_2Cl_2 at -1.31 and -1.65 V versus SCE are most likely also due to $[Py_8TPyzPzH_2]$, although these two redox processes may have underneath some component related to reduction of the dianion ($E_{1/2} = -1.29$ and -1.59 V in CH_2Cl_2, 0.13 M TBA(OH)). In summary, therefore, these results confirm that the neutral and the dianionic species are in equilibrium with each other both in neat CH_2Cl_2 and in pyridine.

Moreover, despite the fact that there is a large majority of one species in each solvent, $[Py_8TPyzPzH_2]$ in CH_2Cl_2 and $[Py_8TPyzPz]^{2-}$ in pyridine, whatever the precise relative amounts of the two species present, they undergo four distinct one-electron reductions and not five as might appear to be the case at first sight from Figure 5. These findings are in good agreement with results of the corresponding metal derivatives of $[Py_8TPyzPzH_2]$, having the formula $[Py_8TPyzPzM]$, which also show four one-electron reductions.[13]

Half-wave potentials for the four reductions of $[Py_8TPyzPzH_2]$ are summarized in Table 4 together with $E_{1/2}$ values of related tetrapyrrolic analogues. The species

Table 4. Half-Wave Potentials (V vs SCE) in CH_2Cl_2, 0.1 M TBAP, of $[Py_8TPyzPzH_2]$, $[Py_8TPyzPz]^{2-}$, and Analogues

	reduction, $E_{1/2}$					$\Delta E_{1/2}$			
compd	1st	2nd	3rd	4th		Δ_{1-2}	Δ_{2-3}	Δ_{3-4}	refs
$[Py_8TPyzPzH_2]$	−0.15	−0.50	−1.31	−1.65		0.35	0.81	0.34	TP[a]
$[PcH_2]$[c]	−0.66	−1.06	−1.93	−2.23		0.40	0.87	0.30	23
$[(t\text{-Bu})_4PcH_2]$[b]	−0.82	−1.19				0.37			21a
$[Ph_8DzPzH_2]$[b]	−0.42	−0.66	−1.02	−1.15	−1.34	0.24	0.36	0.13	7b
$[Py_8TPyzPz]^{2-}$	−0.98	−1.29	−1.45	−1.59		0.31	0.16	0.14	TP[a]
$[Pc]^{2-}$ [c]	−1.24	−1.55	−1.95	−2.23		0.31	0.40	0.27	23

[a] TP: this paper. [b] Solvent: CH_2Cl_2. [c] Solvent: DMF, with $(Pr_4N)ClO_4$ as supporting electrolyte.

$[Py_8TPyzPzH_2]$, due to the presence of the external electron-deficient dipyridinopyrazine fragments, undergoes more facile stepwise reductions than those observed for $[PcH_2]$, its analogue $[(t\text{-Bu})_4PcH_2]$ or $[Ph_8DzPzH_2]$. The first reduction is less negative by ca. 0.50 V as compared to the corresponding $E_{1/2}$ value for free-base phthalocyanine, $[PcH_2]$, and by ca. 0.67 V as compared to the half-wave potential of the phthalocyanine analogue, $[(t\text{-Bu})_4PcH_2]$, which carries electron-donating *t*-butyl groups (see Table 4).

In line with expectation, the $E_{1/2}$ for all four reductions of $[Py_8TPyzPz]^{2-}$ are also more positive than $E_{1/2}$ for the four reported reductions of $[Pc]^{2-}$ (Table 4), but the difference in half-wave potentials ($\Delta E_{1/2}$, Table 4) between each two successive reductions of $[Py_8TPyzPzH_2]$ and $[PcH_2]$ are quite similar to each other, i.e., Δ_{1-2} and Δ_{3-4} range from 0.30 to 0.40 V for both species, while Δ_{2-3} is 0.81 V for $[Py_8TPyzPzH_2]$ and 0.87 V for $[PcH_2]$. These results indicate that the reduction processes of the porphyrazines and the phthalocyanines are the same.

The data in Table 4 clearly show that the first two reductions of $[Py_8TPyzPzH_2]$ are more facile than $E_{1/2}$ for reduction of the diazepinoporphyrazine macrocycle $[Ph_8DzPzH_2]$ which also carries external electron-withdrawing fragments.[7b] Interestingly, however, a reversed situation is found for the third and fourth reductions, since less negative potentials are needed for further electron addition to the diazepinoporphyrazine macrocycle. This is perhaps not surprising if one considers that progressive electron uptake in the latter macrocycle is highly favored by the $6H \rightarrow 1H$ tautomerism which occurs at the electron-deficient diazepine rings, as discussed previously.[7b] Such a type of tautomerism can lead to an increase of the overall planarity of the macrocycle, thus resulting in an extension of the π-electron conjugation, with consequent facilitated electron uptake and excess negative charge redistribution and stabilization.

UV−Vis Characterization of the $[Py_8TPyzPzH_2]$/$[Py_8TPyzPz]^{2-}$ Equilibrium. Spectrally monitored titration experiments on the neutral compound give further evidence that the five redox processes shown in Figure 5 originate from a combined response due to the concomitant presence of two major species in equilibrium with each other, i.e., $[Py_8TPyzPzH_2]$, widely predominant in CH_2Cl_2, and its corresponding dianion $[Py_8TPyzPz]^{2-}$, which is present in pyridine.

In order to confirm this equilibrium given by eq 1, a solution of $[Py_8TPyzPzH_2]$ ($c = 1.02 \times 10^{-5}$ M) obtained

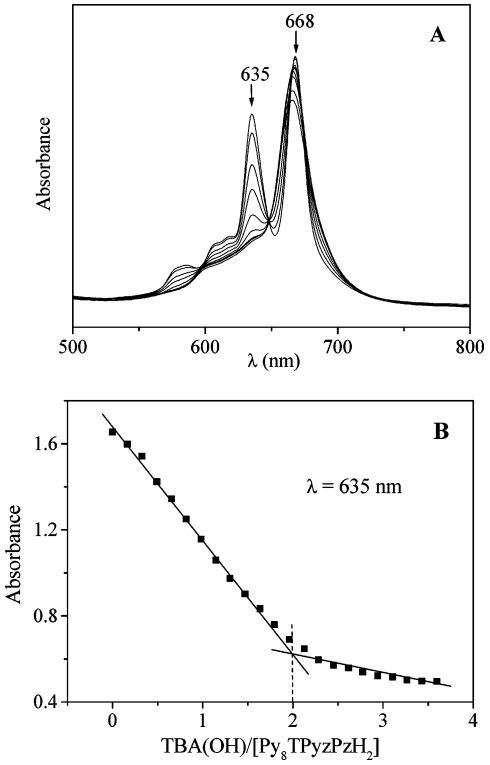

Figure 8. (A) Spectral changes observed during the titration of 1.02×10^{-5} M $[Py_8TPyzPzH_2]$ in CH_2Cl_2 by TBA(OH). (B) Plot of the absorbance (λ = 635 nm) of $[Py_8TPyzPzH_2]$ vs the molar ratio TBA(OH)/$[Py_8TPyzPzH_2]$.

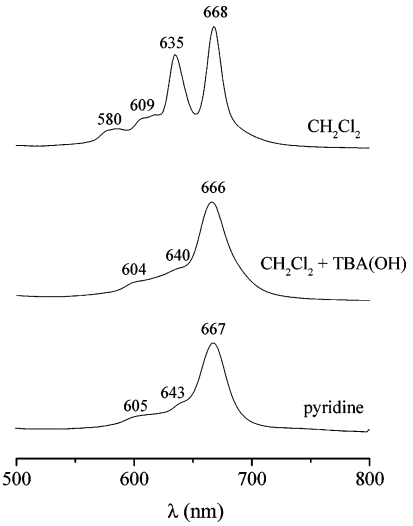

Figure 9. UV−vis spectra of $[Py_8TPyzPzH_2]$ under different solution conditions.

after complete dissolution (1−2 h) of the suspended macrocycle in CH_2Cl_2 was titrated with TBA(OH) at 296 K, and the UV−vis spectrum was taken after each addition.

Figure 8A shows the UV−vis spectral changes which occur upon the addition of 0−4 equiv of TBA(OH) to solution. As TBA(OH) is added, there is an almost complete disappearance of the band at 635 nm (Q_y), whereas the band at 668 nm (Q_x) decreases slightly in intensity and shifts to 666 nm. The final spectrum in CH_2Cl_2 containing 4 equiv of TBA(OH) is indicative of a compound with D_{4h} symmetry and compatible with formation of the dianion $[Py_8TPyzPz]^{2-}$ observed in pyridine. This spectral comparison is illustrated in Figure 9. The presence of a well-defined isosbestic point in the Figure 8A indicates that the $[Py_8TPyzPz]^{2-}$ dianion is formed in the absence of spectrally detectable amounts of intermediates, i.e., the monodeprotonated species $[Py_8TPyzPzH]^-$.

A plot of the absorbance at 635 nm during the titration versus the molar ratio of the two reactants, TBA(OH)/$[Py_8TPyzPzH_2]$, is given in Figure 8B. Two straight lines with different slopes are obtained, which intersect at a mole ratio of ca. 2:1 as expected for a 2:1 molar ratio TBA(OH)/$[Py_8TPyzPzH_2]$. This result is consistent with a titration of two protons from $[Py_8TPyzPzH_2]$ as shown in eq 7.

$$[Py_8TPyzPzH_2] + 2OH^- \rightleftarrows [Py_8TPyzPz]^{2-} + 2H_2O \quad (7)$$

The final spectrum in Figure 8A has the same shape and the same maximum wavelength as the spectrum of $[Py_8TPyzPzH_2]$ in pyridine (Figures 3D and 9). This further confirms that the species mostly present in pyridine is the dianion $[Py_8TPyzPz]^{2-}$ (neutralized by pyridinium cations). Formation of a dianion has also been observed in pyridine for the unmetalated thia-[5a] and selenodiazolporphyrazines[6a] as well as for diazepinoporphyrazine[7a] and for other porphyrazine analogues.[3] In contrast, deprotonation of the macrocycle does not occur for the related phthalocyanine, $[PcH_2]$, which shows a split Q band in this solvent, as discussed in ref 5a and references therein.

Evidently, the replacement of the benzene rings in $[PcH_2]$ by annulated electron-deficient heterocyclic rings in $[Py_8TPyzPzH_2]$ highly polarizes the central NH groups, thus facilitating their dissociation. An indication of the strong polarization of the central ($N^{(\delta-)}H^{(\delta+)}$) groups in $[Py_8TPyzPzH_2]$ and its facile dissociation is further indicated by the fact that the dianionic $[Py_8TPyzPz]^{2-}$ is also formed in solvents of progressively lower donor capability than pyridine, i.e., DMSO, DMF, and CH_3CN (unsplit Q band), whereas a splitting of the Q band is seen in the low donor C_6H_5CN, due to the presence of the neutral species, as occurs in CH_2Cl_2 and $CHCl_3$ (Table 3).

Spectroelectrochemical Measurements. Figure 10 shows the UV−vis spectral changes which occur upon the first and second one-electron reductions of $[Py_8TPyzPzH_2]$ in pyridine where the species in solution is the dianion $[Py_8TPyzPz]^{2-}$. During controlled-potential thin-layer reduction (second scan, potential fixed at −0.30 V), the neutral species $[Py_8TPyzPzH_2]$ is progressively reduced to $[Py_8TPyzPzH_2]^-$. The UV−vis spectrum in Figure 10A shows the following changes: (i) a significant decrease in intensity and broadening of the Q band at 667 nm, (ii) a shift of the B band position from 361 to 342 nm, (iii) an increase in intensity of the peak located just above 400 nm, and (iv) the appearance of new peaks at 554, ca. 890 (broad), and 987 nm. It is noteworthy that the final spectrum belonging to the monoanion $[Py_8TPyzPzH_2]^-$ is practically identical to the spectrum obtained after the first one-electron reduction of $[Py_8TPyzPzH_2]$ in CH_2Cl_2 to give $[Py_8TPyzPzH_2]^-$ (not shown). Formation of this paramagnetic species in pyridine

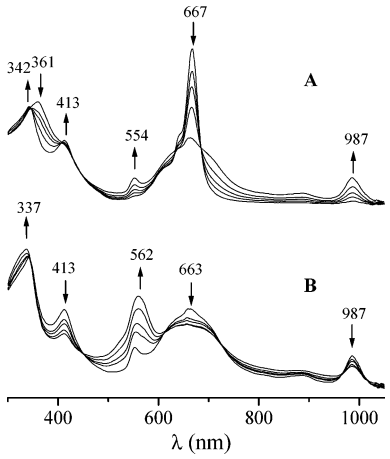

Figure 10. UV−vis spectral changes in pyridine containing 0.2 M TBAP during controlled-potential electrolysis of $[Py_8TPyzPzH_2]$ at (A) −0.30 V (first reduction, second scan), (B) −0.70 V (second reduction, second scan).

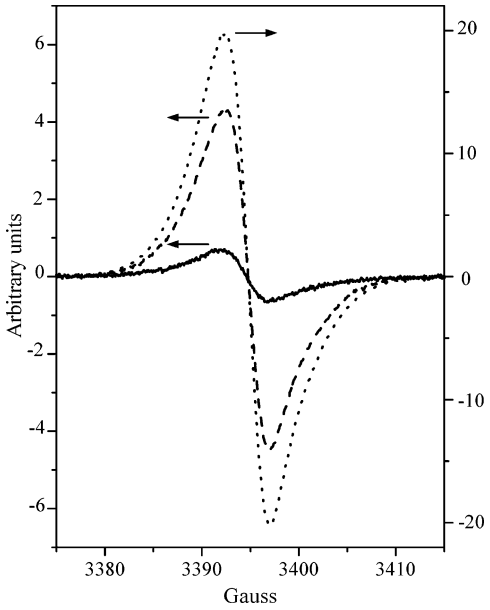

Figure 11. Low-temperature (77 K) EPR spectra of $[Py_8TPyzPzH_2]$ (present as the dianionic species $[Py_8TPyzPz]^{2-}$) in pyridine containing 0.2 M TBAP (g = 2.003; scan range 100 G): - - -, after first reduction at controlled-potential (−0.30 V); —, after second reduction (−0.70 V), and then ···, after back one-electron reoxidation (−0.30 V, intensity on the right scale coherent with the left one).

is confirmed by the appearance in the EPR spectrum of a narrow peak at g = 2.003 (Figure 11, curve - - -) indicative of the presence of a π-anion radical.

Well-defined UV−vis spectral changes are also seen in pyridine upon the second one-electron reduction of $[Py_8TPyzPzH_2]^-$ to give $[Py_8TPyzPzH_2]^{2-}$ (see Figure 10B). These spectral changes are as follows: (i) a decrease in intensity in the peaks at 413 and 987 nm and (ii) a marked increase in intensity of the peak at 554 nm, which is slightly shifted to 562 nm. Less significant changes are observed for the peak at ca. 337 nm and for the band centered at ca. 660 nm. The EPR spectrum of $[Py_8TPyzPzH_2]^{2-}$ (Figure 11, curve —) shows only a weak signal due probably to some residual presence of $[Py_8TPyzPzH_2]^-$, thus indicating that $[Py_8TPyzPzH_2]^{2-}$ contains no unpaired electrons; i.e., it is diamagnetic, in line with expectation.

The spectral changes which accompany the stepwise reoxidation of $[Py_8TPyzPzH_2]^{2-}$ in pyridine lead to a full regeneration of the initial spectrum belonging to the dianion $[Py_8TPyzPz]^{2-}$. The one-electron reoxidation of $[Py_8TPyzPzH_2]^{2-}$ (Figure 11, curve ···) also fully regenerates the EPR spectrum of the π-anion radical $[Py_8TPyzPzH_2]^-$ (the higher intensity of the peak is easily explained on the basis of a more concentrated solution at the time of reoxidation).

Parallel UV−vis changes are observed in CH_2Cl_2 upon the stepwise reoxidation from $[Py_8TPyzPzH_2]^{2-}$, the final spectrum belonging to the neutral $[Py_8TPyzPzH_2]$ (split Q-band). The above facts confirm the complete reversibility of the first two one-electron redox processes in both solvents. Well-defined isosbestic points obtained throughout the forward and reverse two-electron exchange processes further support the well-defined uptake and release by the macrocycle of the first and second negative charge units.

Conclusions

A new pyrazinoporphyrazine macrocycle, i.e., tetrakis 2,3-[5,6-di(2-pyridyl)pyrazino]porphyrazine (hydrated), $[Py_8TPyzPzH_2]\cdot 2H_2O$, has been isolated in good yield by a one-step synthetic reaction involving the direct cyclotetramerization of its precursor, 2,3-dicyano-5,6-di(2-pyridyl)-1,4-pyrazine, $[(CN)_2Py_2Pyz]$, in the presence of DBU. Due to aggregation phenomena, colloidal dispersions of the macrocycle in different solvents are formed which, with time, evolve to give clear solutions containing exclusively the monomeric form of the macrocycle, either preponderantly present as the neutral species $[Py_8TPyzPzH_2]$ (in $CHCl_3$, CH_2Cl_2, and CH_3COOH) or as its corresponding dianion $[Py_8TPyzPz]^{2-}$ (in pyridine). Titration of a $[Py_8TPyzPzH_2]$ solution in CH_2Cl_2 with TBA(OH) establishes that the macrocycle undergoes an overall two-proton loss and behaves as a strong acid. These somewhat exceptional acidic properties are explained on the basis of the quite remarkable electron-withdrawing capacity expressed by the external dipyridinoporphyrazine fragments. Electrochemical and spectroelectrochemical data, in comparison with that of phthalocyanine and related porphyrazine analogues, provide clear evidence that the electron uptake, upon the reversible multiple step reduction, is greatly facilitated by π-electron accumulation and charge redistribution. As will be shown in the following paper,[13] a rich electrochemical behavior is also exhibited by metal complexes having the formula $[Py_8TPyzPzM]$ (M = bivalent nontransition and first-row transition metal ion).

Acknowledgment. Financial support by the University of Rome La Sapienza and the MIUR (Cofin 2003038084) and the Robert A. Welch Foundation (K.M.K, Grant E-680) is gratefully acknowledged. M.P.D. is indebted to the Department of Chemistry, Houston University, for generous help and kind hospitality. Thanks are expressed to Dr. P. A. Stuzhin (Ivanovo State University of Chemical Technology, Ivanovo, Russia) for critical comments and helpful sugges-

tions and to Dr. Paola Galli and Dr. Jianming Lu for great experimental support.

Supporting Information Available: X-ray crystallographic files in CIF format for the structure determination of 2,3-dicyano-5,6-di(2-pyridyl)-1,4-pyrazine. ORTEP views of molecules A and B (Figures S1 and S2), FAB (Figure S3), IR spectrum (Figure S4) and X-ray powder pattern (Figure S5) of [$Py_8TPyzPzH_2$]. This material is available free of charge via the Internet at http://pubs.acs.org.

IC048909W